HiSST: 2nd International Conference on
High-Speed Vehicle Science Technology
11–15 September 2022, Bruges, Belgium

Investigation of Flame Stabilization and Combustion mode in a Hydrogen Fueled Scramjet Combustor using LES-PaSR Numerical Simulation

Seung-Min Jeong[1], *Jeong-Yeol Choi*[1]

Abstract

In our previous study, we conducted a two-dimensional delayed detached eddy simulation (DDES) high-resolution numerical simulation on a laboratory-scale direct-connect hydrogen-fueled scramjet combustor[1]. In this study, sampling data was accumulated up to 100 ms(millisecond) at each global equivalence ratio case. The numerical results showed the formation/propagation/dissipation of pressure and shock wave, so-called the "upstream-traveling shock wave", induced by complex heat release in the combustor. It was confirmed that this low-frequency combustion instability has order of 100 Hz, and major instability frequency was shifted depending on changing of global equivalence ratio. Dynamics of major instability frequency is derived identically from several experimental studies. The previous numerical study showed underlying physics of low-frequency combustion instability on scramjet combustor, however it has limitation, two-dimensional study. Therefore, in present study, three-dimensional improved delayed detached eddy simulation (IDDES) with detailed laminar chemical mechanism and partially stirred reactor (PaSR) model was performed to investigate more detailed dynamics of low-frequency instability on scramjet combustor as preliminary staged. For high-resolution, convective and viscous fluxes were handled by high-order accurate multi-dimensional limiting scheme. Through comparison with supersonic co-axial jet experimental results, the constructed three-dimensional LES-PaSR numerical framework has high-fidelity. The simulation was conducted under two global equivalence ratio conditions of 0.35 and 0.45. Results showed dynamic of detailed reactive flow-field, and flame structure. A results of counter-rotating vortex pair (CRVP) shape inform that the effect of different fuel injection pressure on fuel/air mixing process and forming of entire reactive flow-filed of scramjet combustor. Based on present preliminary numerical study, series of comprehensive numerical simulation will be performed with tremendous sampling time up to 30 ms.

Keywords (Tahoma 10 pt, bold): *Scramjet combustor, Numerical simulation, High-order accurate, Improved Delayed Detached Simulation (IDDES), Global equivalence ratio.*

1. Introduction

During the last decade, scramjet technologies have been advanced for the level of real-world application. However, it was revealed that several issues for further development. One of these is combustion instability. Because incoming air or vitiated air has extremely high speed, flow residence time at the combustor section is very short and is an order of 0.1 ms (millisecond). This phenomenon made the early scientific community belief which is that combustion oscillation or acoustic wave cannot exist and easily exhaust from the combustor. However, several experimental, numerical, and theoretical studies break this belief and showed the clue that combustion oscillation are obviously existed as different types depending on the chemical composition of the fuel, fueling schemes, shape, and operating condition of a scramjet combustor[2-9].

Choi et al.[2,3] conducted numerical simulation on the HyShot test model with various fuel injection and shape conditions. This study exhibited that the combustion oscillation is existed very nature

[1] *Department of Aerospace Engineering, Pusan National University, Busan 46241, Korea)*

characteristics at nominal operating conditions in a hydrogen-fueled scramjet engine. Ma et al.[4] and Lin et al.[5] performed comprehensive study on ethylene-fueled scramjet combustor including numerical, experimental, and theoretical approaches. In these series of studies, combustion instability was detected under the various fueling schemes, and major instability frequency was increased when the global equivalence ratio was increased. Micka et al.[6] conducted an experimental study on ethylene-fueled dual-mode scramjet. Through the various fueling schemes and operating conditions, they characterized local combustion mode depending on each condition. Especially, this study reported that strong combustion instability was encountered when the operating mode changed from ram to scram mode. The experimental study of Wang et al.[7] showed the flame flash-forward and blow-off dynamics at the region near the injector side on an ethylene-fueled scramjet combustor. And they reported that these dynamics occurred repetitively and derived major frequencies about 200 Hz to 400 Hz. Nakaya et al.[8] performed an experimental study on ethylene-fueled scramjet combustor and analyzed the experimental results using imaged-based dynamic mode decomposition (DMD). The results showed two types of events, the cavity shear-layer combustion oscillation and the jet-wake type combustion instability. The study by Jian et al.[9] exhibited the engine surging under ram-mode operating at the general flight condition due to strong combustion instability. Furthermore, in this study, they conducted a simple but clear numerical simulation to show the dynamics of upstream-traveling shock waves (UTSW) generated by continuous heat release. These simple results informed the importance of controlling the upstream-traveling shock waves in terms of achieving the stabilization of engine operation and avoiding the inlet unstart. These studies inform that the combustion oscillation and instability are existed in a scramjet engine with various dynamics. And, it can be seen that focusing on low-frequency range is important to investigate dynamics of combustion instability. However, it is tough to extract details of each local property from the experimental approach due to the limitations of the measurement method. Therefore, there is no way but to solve the entire process numerically to reveal the reactive flow-field dynamics of a scramjet engine. Because of required sampling time is about over the tens millisecond to capture the repetitive dynamics of the low-frequency range, conducting a case study using a three-dimensional numerical approach is not easy and challenging.

In this context, we performed two-dimensional high-resolution numerical simulation on the hydrogen-fueled direct connect scramjet combustor as the initial step of investigate low-frequency combustion instability on high-speed air-breathing vehicle [1]. This previous numerical study achieved sampling time up to 100 ms at total five global equivalence ratio cases. In a high equivalence ratio condition, repetitive motion of the upstream-traveling shock waves was detected. These repetitive dynamics have a period of several milliseconds and were captured during the entire time range. This upstream-traveling shock waves affect periodically on fuel/air mixing and burning process, generating the low-frequency combustion instability. The results of the previous study revealed the underlying physics of the combustion instability on a scramjet combustor. However, because of this simulation is based on two-dimensional, investigating the detailed mechanism has limited. To avoid this limitation, in the present study, three-dimensional high-resolution hybrid LES/RANS numerical simulation with detailed chemical mechanism was conducted. The computational domain consisted of 60.6 million grid points, referring to the grid convergence test in the previous study. The framework applied the algebraic PaSR model to treat the turbulent-combustion interaction. Two of global equivalence ratio condition was considered. The target sampling time of the present simulation is about 30.0 ms. However, the present study will focus on instantaneous field data after 5 flow through time (FFT) when the fuel injection started.

2. Numerical approach and Combustor model

2.1. Numerical methodology

In the present simulation, a density-based fully compressible reactive in-house solver, called "PNU-RPL3D", was used. The governing equation has a fully coupled form of chemical conservation, momentum, energy, and turbulent transport equation and was resolved by the finite volume method (FVM). The ideal gas equation of state was used to calculate pressure. Density was handled by the sum of each species partial density. SST-IDDES model, which was suggested by Gritskevich et al.[10] was applied for resolving turbulent motion. Jachimowski hydrogen/oxygen detailed laminar chemical mechanism [11], which consists of 8 species and 25 reaction steps, was used for chemistry. Total 9 species were considered, including nitrogen as an inert gas. A simple algebraic PaSR model [12] was applied to consider turbulent-combustion interaction in the sub-grid scale. The simple algebraic PaSR

model has several uncertainties, such as calculating the chemical time scale, correcting high-Mach number cases, and selecting the model constant [13~15]. The study by Peterson et al.[13] which is conducted three-dimensional numerical simulation on round supersonic combustor, clearly showed the sensitivity of PaSR model constant. The results illustrated quite different anchored locations of the pre-combustion shock depending on the model constant. To avoid this uncertainty and achieve a solid result with the PaSR model, a comprehensive study on the modeling of PaSR for high-speed combustion problems seems to be needed. However, the study by Gonzalez-Juez et al.[16] reported that the effect of the turbulent-combustion model is minute when performing the simulation with 1. detailed chemistry, 2. sufficiently high-resolution on small volume combustor(less than O(1,000 cm3)). The present scramjet combustor has an O(100 cm3) volume. Furthermore, considering that supersonic combustion dominates the reactive flow field of the present scramjet combustor, it can be acceptable to apply an empirical form of the PaSR model. In fact, the PaSR coefficient of the present study is around 0.95~0.99. It means that the effect of the turbulent-combustion model is very minute, and the PaSR results are almost identical to the results of "no-model approach". To guarantee high-fidelity and high-resolution, convective and viscous flux was handled by 5th order optimized multi-dimensional limiting process (oMLP)[17] and 4th order central difference. Because a based on interpolation of multi-dimensional convective properties, the oMLP scheme has much better performance than essentially non-oscillatory (ENO) family schemes, such as WENO, TENO[18,19]. The RoeM flux splitting scheme is used in the present study. The 2nd order fully implicit optimized lower-upper symmetric gauss-seidel (LU-SGS)[20] is used for time integration. Each time step has a maximum of six stages of sub-iteration. Every sub-iteration has convergence criterion of less than 1 %. The framework is parallelized by a message passing interface (MPI) with blocking communication. The experimental set-up is currently under the verify a design points. Therefore code validation was conducted using co-axial supersonic jet problem which was performed by Evans et al.[21]. The results showed a quite good agreement with experimental data, so present numerical framework has high-fidelity. Detailed comparison results are noted in reference[1,18].

2.2. Computational domain

The computational model, PNU-DCSC (direct connect scramjet combustor) is illustrated in Fig. 1. This PNU-DCSC consist of vitiated air heater (VAH), shape transition nozzle[22] and scramjet combustor. The vitiated air heater is very similar shape with the Penn. state university's rocket combustor model-1 (RCM-1) which was conducted experimental test by Marshall et al.[23]. A design point of the scramjet combustor is that main flow at the isolator inlet has Mach number of 2.0 and temperature of 1,000 K. The isolator has a constant cross-sectional area of 20 x 20 mm^2. Present study has two different fuel injection condition depending on global equivalence ratio, 0.35 and 0.45.

Computational domain consist of the isolator and combustor. Vitiated air is coming most left side of the computational domain. The present combustor has the same width and height in the isolator. Therefore, we can get a three-dimensional computational region by imposing same grid point in z-direction, referring the grid convergence results from previous two-dimensional study[1]. Total number of domains is 1,034 and each block has exactly same grid resolution of 13×73×73. Present study has about 71.6 million grid point with structure grid topology. Adiabatic, non-catalytic, non-slip boundary condition was imposed at all walls excepted fuel injector.

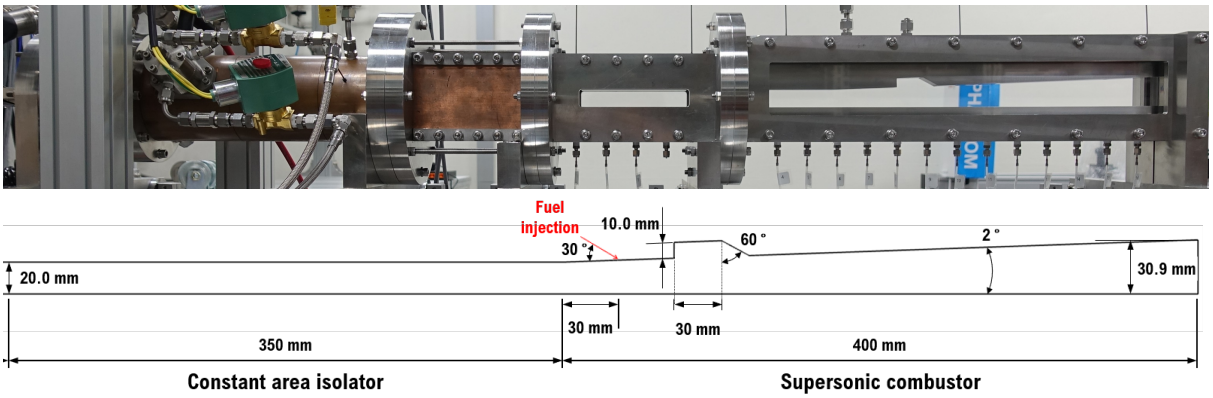

Fig 1. (top) Configuration of experimental set-up and (bottom) schematic of computational domain

Table 1. Incoming vitiated air and fuel injection condition

		Isolator inlet (nozzle exit)	**Fuel injection $\Phi \approx 0.35$**	**Fuel injection $\Phi \approx 0.45$**
Mach number		2.05	Sonic condition	Sonic condition
Temperature		1,000 K	291.15 K	291.15 K
Pressure		1.8 bar	4.0 bar	5.2 bar
Mass fraction	N_2	60.5	-	-
	O_2	21.1	-	-
	H_2O	18.4	-	-
	H_2	-	100	100

3. Numerical results

The process and stabilization time of formation of supersonic flow fields were checked firstly to inject fuel after the supersonic flow field is sufficiently stabilized. The supersonic flow field was fully stabilized at 4.0 ms after the VAH was started. Based on this result, fuel was allowed to be injected after this moment. All data illustrated in the present study are instantaneous results in which 5 flow through time (FTT) after the fuel is injected. In the present condition, 1 FFT is about 0.2 ms. It means that the present study's reactive flow-field data is not the flame stabilized results but represents information from the stabilized process.

3.1. Flame structure depending on each global equivalence ratio

The instantaneous results of each property depending on the two global equivalence ratios are depicted in Fig. 2. Both global equivalence ratio cases present the jet-wake type combustion mode. The normalized heat release rate (HRR) of the present study was calculated by the reaction rate and the heat of formation of all species involved in a chemical process. HRR is distributed not only in a shear layer aligned from the cavity front wall to the cavity-closeout location but also outermost of the fuel/air mixing layer. HRR also shows a strong distribution at the re-circulation region and the upper wall surface right before and after the injector. However, strong HRR is reduced in the region between the injector and the cavity. Therefore, the combustion mode of these two cases is not complete jet-wake combustion mode, but the cavity assisted jet-wake combustion mode. At the downstream of the combustor, HRR was no more detected in the core of the fuel/air stream, but only outermost of the stream.

The changing of dynamics on temperature, pressure and HRR inform a compressible effect on supersonic reactive flow field of scramjet combustor. In both equivalence ratio case, the fuel stream is kept an unburnt state at the region before the cavity-closeout. A temperature field of less than about 1000 K appears in this area. This cold fuel stream rapidly rises in temperature as it passes through the cavity-closeout region, and an about 2500 K distribution appears in the downstream of the combustor. The pressure field presents quite different dynamics. In the higher equivalence ratio case, at the region of 41.8 cm away from the isolator inlet, it shows that high pressure distribution forming due to complex interaction between a shock structure induced by fuel injection and the acoustic oscillation of the cavity. This complex dynamics of the shock and pressure wave forms a pressure field of about up to 0.3 MPa at the area. This high-pressure structure is form at non-reactive region, therefore, it can be seen that the compressibility has more affect rather than the chemical reaction process on forming the high-pressure distribution. At the region of 47.0 cm away from the isolator inlet, the compressibility effect become more enhanced. The combustion was held mainly along the fuel/air mixing layer. Mixing layer was growth during it passed the cavity-closeout region. When this mixing layer impinged at the rear wall of the cavity which has angled, the mixing layer was highly affected and taken highly suppressed. This process lead that anchoring the maximum pressure of the combustor on the lower wall of the cavity-closeout region and inducing pressure drop on the behind of the cavity rear wall.

Both cases illustrated that the fuel/air stream re-accelerated over sonic speed while it passed the cavity-

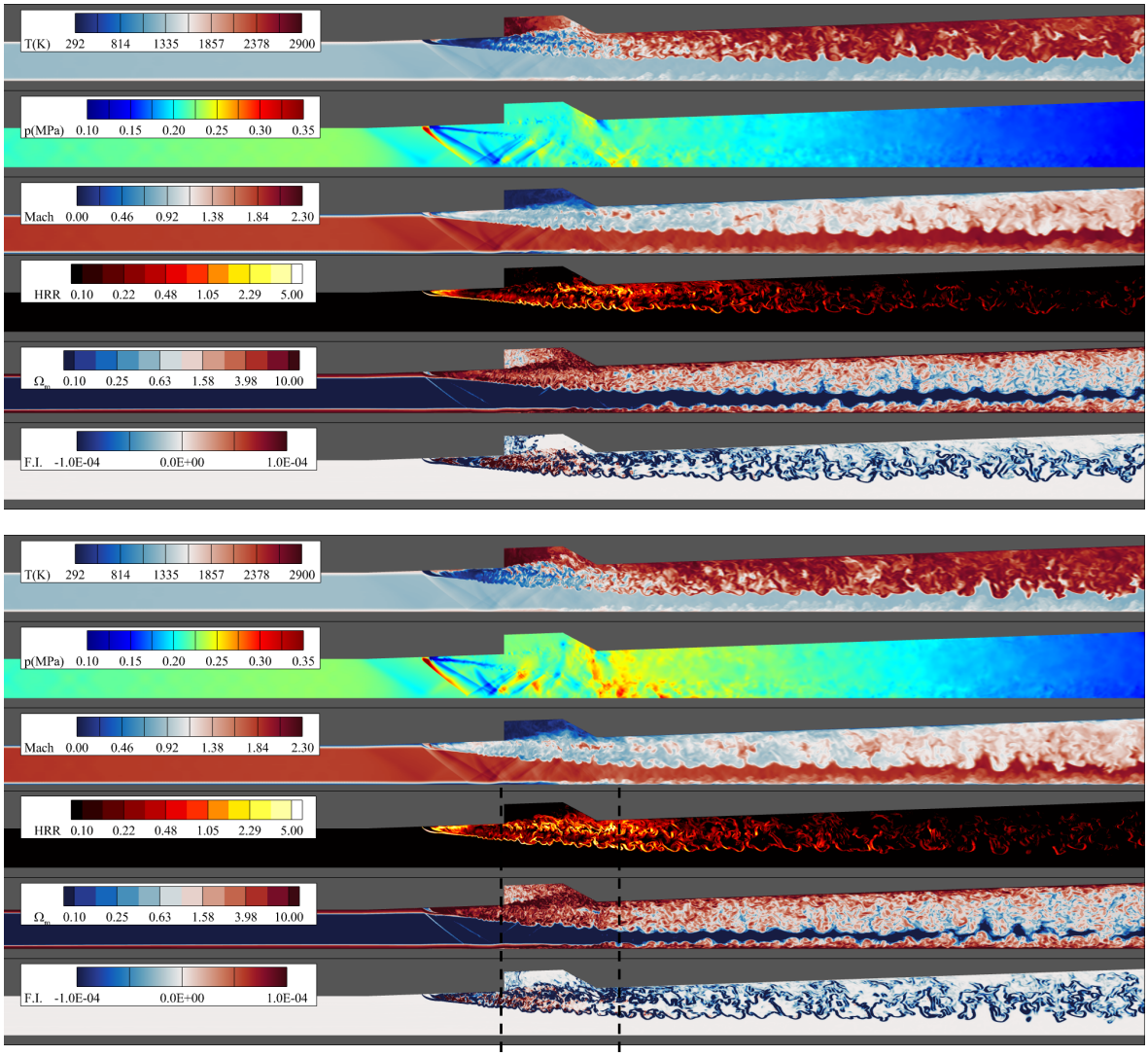

Fig 2. Instantaneous results of temperature, pressure, Mach number, normalized heat release rate, vorticity and flame index distribution at the y-center plain; (top) $\Phi \approx 0.35$, (bottom) $\Phi \approx 0.45$

closeout region. The location where the stream accelerated over the sonic speed is slightly shifted downstream of the combustor due to the different fuel injection pressure. The flame index results indicated that the non-premixed flame characteristics dominate the cavity-closeout region, and the premixed flame characteristics govern the other region.

The change of the flame structure depending on the global equivalence ratio can be investigated in Fig. 3. The dotted line and solid line indicate the properties at the front and rear wall of the cavity, respectively. The quantity of the maximum temperature is almost identical in both global equivalence ratio conditions. However, the anchored region of the maximum temperature is quite different. In the lower equivalence ratio, the maximum temperature is held at about 0.7 along the normalized height direction, whereas the maximum temperature is anchored at a point of about 0.5 in the higher equivalence ratio case. These results show that flame surface dynamics depend on changing equivalence ratios. The OH mass fraction and HRR also indicate strong distribution on the outermost of the fuel/air mixing layer rather than the core. It can be founded that the non-premixed flame characteristics dominate after the cavity-closeout region, as depicted in the flame index results in Fig. 3. The changing of quantitative distribution informs that most reaction process is held in the mixing layer of the fuel/air stream. Because of using the instantaneous results, it is somewhat difficult to classify the detailed flame structure depending on the equivalence ratio changed, but it can be expected

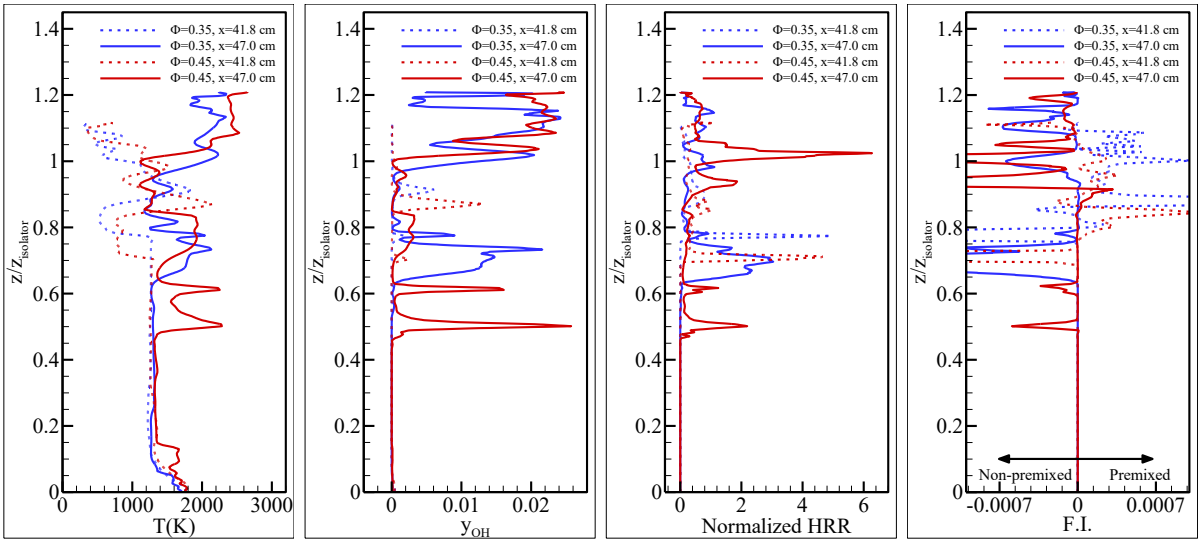

Fig 4. Temperature, OH mass fraction, normalized heat release rate and flame index distribution extracted along the y-center plane; (dot line) 41.8 cm (solid line) 47.0 cm

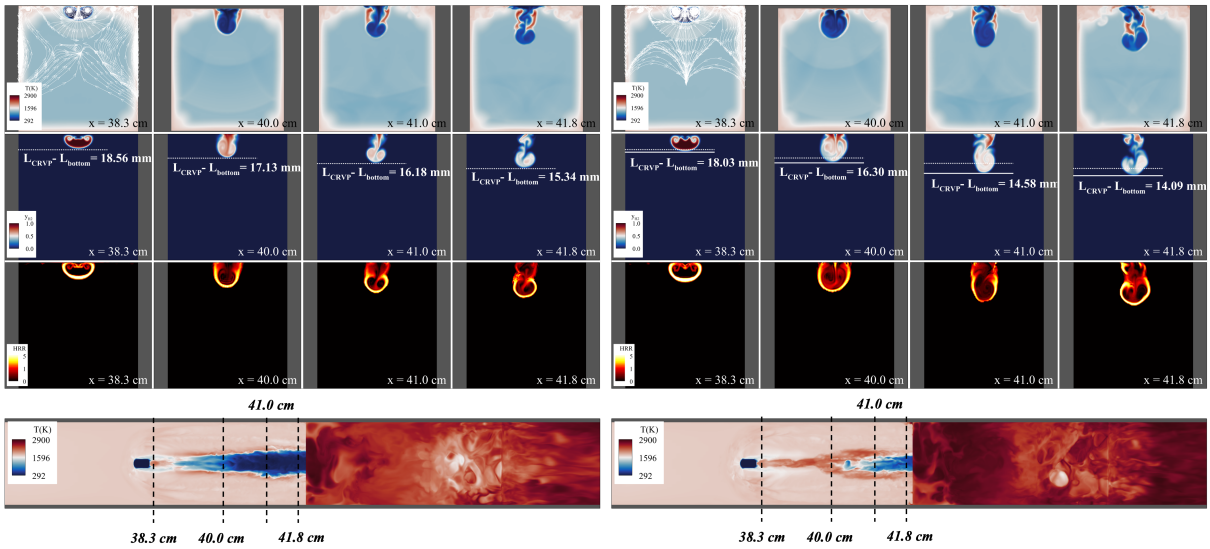

Fig 3. The instantaneous results at the region between the fuel injector and the front wall of the cavity; (top) the temperature, H2 mass fraction and normalized HRR results at each x-plane, (bottom) the temperature results on the top of the z-plane.

to take more detailed results if using the time-averaged results in a follow-up stage. The different fuel injection pressure induces the fuel penetration length and changes the flame surface anchored location, as demonstrated in Fig. 3.

Fig. 4 illustrates the instantaneous temperature distribution on the top wall near the fuel injector and the counter-rotating vortex pair (CRVP) dynamics under the different global equivalence ratios. The equivalence ratio of 0.35 case appeared the circular shape CVRP. The velocity streamlines result indicated that the injected fuel cannot significantly affect the vitiated air stream. Therefore, the equivalence ratio of 0.35 case has a short penetration length, resulting in the CVRP and fuel stream not being detached from the top wall surface sufficiently. The equivalence ratio of 0.45 case has an oval shape CVRP, and the velocity streamline shows that injected fuel and air stream interact. Therefore, the penetration length is increasing, and the fuel stream is much more detached from the top wall surface than in the lower equivalence ratio case. In both cases, a combustion process is held on the outermost of the CVRP. And due to re-circulation region, burnt gas of the outermost CVRP is trying to

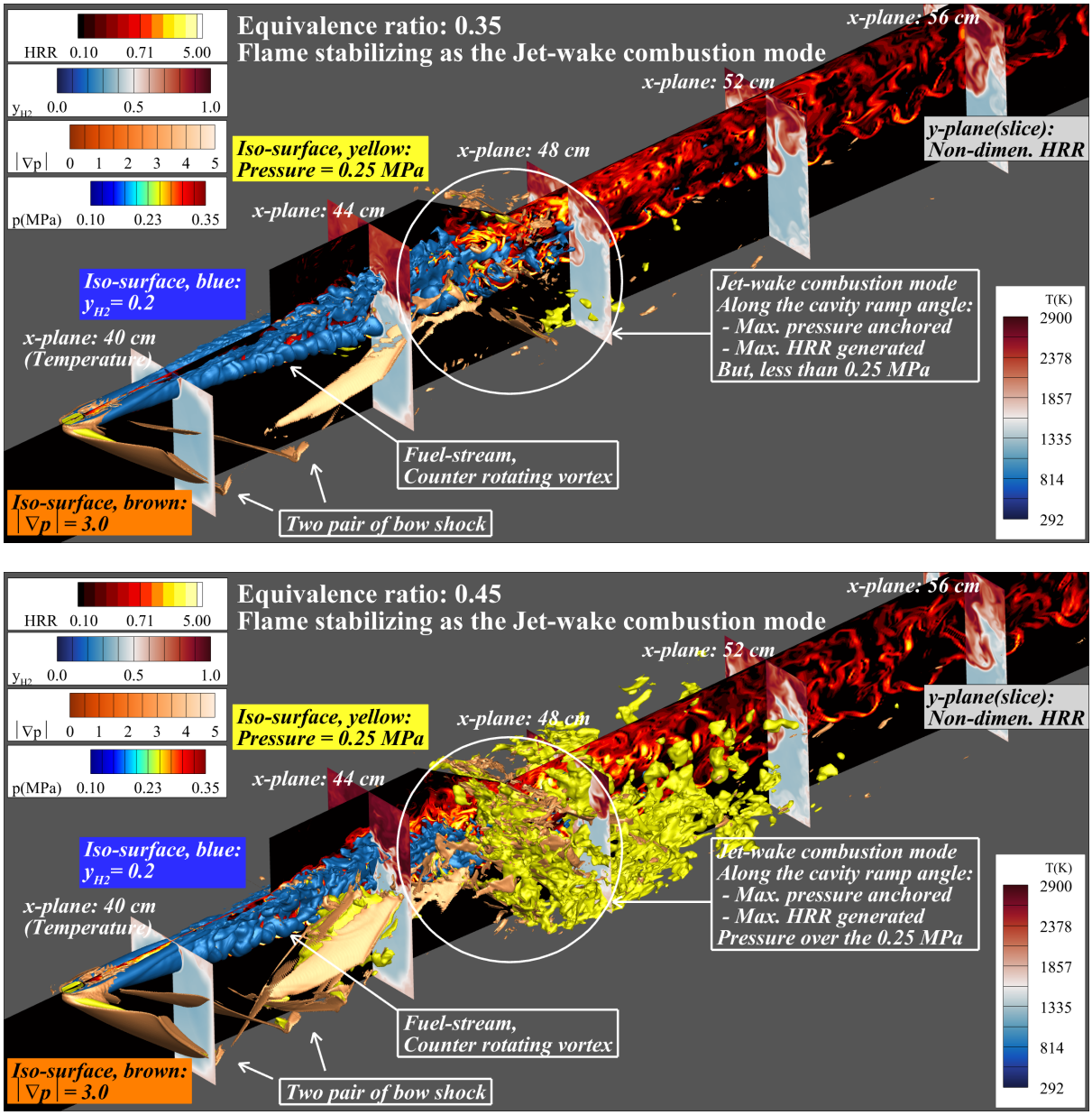

Fig 5. The instantaneous results of reactive flowfield depending on each global equivalence ratio

come into the core of the fuel stream. However, because the top wall acted as a bulkhead, burnt gas outside the fuel stream could not be re-circulated into the core, and lower temperature distribution was appeared on the top wall surface. The HRR contour in Fig. 4 well demonstrates this process. Unlike this, the burnt gas of the outermost region at the higher equivalence ratio case can re-circulate and come into the core of the fuel stream. These dynamics enhanced a mixing and burning and collapse the coherent structure of the injected fuel stream.

Fig. 5 shows that the effect of the injection pressure on the forming reactive flowfield of the scramjet combustor. Two pair bow shock generated by fuel injection, reflected by lower wall, resulting in highly disturbance on fuel stream. In the higher equivalence ratio case, the reflected bow shocks have strong intensity rather than lower case. Therefore, the break-up of the fuel stream accelerated and, mixing and burning process more enhanced than the lower equivalence ratio case. Finally, up to about 0.25 MPa was formed into the cavity-closeout region. These results suggests that both penetration length and shock structure induced by the fuel injection pressure play important role on the reactive flowfield of the scramjet combustor.

References

1. Jeong, S.-M., Lee, J.-H., Choi, J.-Y.: Numerical investigation of low-frequency instability and frequency shifting in a scramjet combustor. Proc. Combust. Inst. 39 (in press, article accepted for publication, 31 Jul 2022)
2. Choi, J.-Y., Ma, F., Yang, V.: Dynamic combustion characteristics in scramjet combustors with transverse fuel injection, 41st AIAA/ASME/SAE/ASEE Joint Propulsion Conference & Exhibit, AIAA 2005-4428 (2005)
3. Choi, J.-Y., Ma, F., Yang, V.: Combustion oscillations in a scramjet engine combustor with transverse fuel injection, Proc. Combust. Inst. 30, 2851-2858 (2005)
4. Ma, F., Li, J., Yang, V., Lin, K.-C., Jackson, T.: Thermoacoustic flow instability in a scramjet combustor, 41st AIAA/ASME/SAE/ASEE Joint Propul. Conf. & Exhibit, AIAA 2005-3824 (2005)
5. Lin, K.-C., Jackson, K., Behdadnia, R., Jackson, T., Ma, F., Yang, V.: Acoustic characterization of an ethylene-fueled scramjet combustor with a cavity flameholder. J Propul. Power 26, 1161–1170 (2010)
6. Micka, D. J.,Driscoll, J. F.: Combustion characteristics of a dual-mode scramjet combustor with cavity flameholder. Proc. Combust. Inst. 32, 2397–2404 (2009)
7. Wang, Z.-G., Sun, M.-B., Wang, H.-B., Yu J.-F, Liang J.-H., Zhuang F.-C.: Mixing-related low frequency oscillation of combustion in an ethylene-fueled supersonic combustor. Proc. Combust. Inst. 35, 2137-2144 (2015)
8. Nakaya, S., Yamana, H., Tsue, M.: Experimental investigation of ethylene/air combustion instability in a model scramjet combustor using image-based methods. Proc. Combust. Inst. 38, 3869–3880 (2021)
9. Jiang, Z., Zhang, Z., Liu, Y., Wang, C., Luo, C.: Criteria for hypersonic airbreathing propulsion and its experimental verification. Chinese J. Aeronaut 34, 94–104 (2021)
10. Gritskevich, M. S., Garbaruk, A. V., Menter, F. R.: Fine-tuning of DDES and IDDES formulations to the k-ω shear stress transport model. Prog. Flight Phys. 5, 23–42 (2013)
11. Singh, D. J., and Jachimowski, C.J.: Quasiglobal Reaction Model for Ethylene Combustion. AIAA Journal 32(1), 213-216 (1994)
12. Evans, M. J., Petre, C., Medwell, P. R., Parente, A.: Generalisation of the eddy-dissipation concept for jet flames with low turbulence and low Damköhler number. Proc. Combust. Inst. 37, 4497–4505 (2019)
13. Li, Z., Ferrarotti, M., Cuoci, A., Parente, A.: Finite-rate chemistry modelling of non-conventional combustion regimes using a Partially-Stirred Reactor closure: Combustion model formulation and implementation details. Appl. Energ. 225, 637–655 (2018)
14. Wu, K., Zhang, P., Fan, X.: On jet-wake flame stabilization in scramjet: A LES/RANS study from chemical kinetic and fluid-dynamical perspectives. Aerosp. Sci. Technol. 120, 107255-107267 (2021)
15. Peterson, D. M.: Simulation of a round supersonic combustor using wall-modeled large-eddy simulation and partially-stirred reactor models. Proc. Combust. Inst. 39 (in press, article accepted for publication)
16. Gonzalez-Juez, E. D., Kerstein, A. R., Ranjan, R., Menon, S.: Advances and challenges in modeling high-speed turbulent combustion in propulsion systems. Prog. Energ. Combust. 60, 26–67 (2017)
17. Kim, S., Lee, S., Kim, K.H.: Wavenumber-extended high-order oscillation control finite volume schemes for multi-dimensional aeroacoustic computations. J. Comput. Phys. 227 4089–4122 (2008)

18. Choi, J.-Y., Unnikrishnan, U., Hwang, W.-S., Jeong, S.-M., Han, S.-H., Kim, K.H., Yang, V.: Effect of fuel temperature on flame characteristics of supersonic turbulent combustion. Fuel (in press, article accepted for publication)
19. Jeong, S.-M., Um, J.-R., Choi, J.-Y.: Numerical study of high resolution schemes for GH2/GO2 rocket combustor using single shear coaxial injector. J. Korean Soci. Propul. Engi. 22(6), 72-83 (2018)
20. Jang, K.-J., Kim, J.-K., Cho, D.-R., Choi, J.-Y.: Optimization of LU-SGS code for the acceleration on the modern microprocessors. Int. J Aeron. Space Sci. 14, 112–121 (2013)
21. Evans, J.S., Schexnayder, C.J.: Influence of chemical kinetics and unmixedness on burning in supersonic hydrogen flames, AIAA J. 18, 188-193 (1979)
22. Sung, B.-K., Choi, J.-Y.: Design of a Mach 2 shape transition nozzle for lab-scale direct-connect supersonic combustor. Aerosp. Sci. Technol. 106906-106018 (2021)
23. Marshall, W., Pal, S., Woodward, R., Santoro, R.: Benchmark wall heat flux data for a GO2/GH 2 single element combustor. 41st AIAA/ASME/SAE/ASEE Joint Propulsion Conference & Exhibit, AIAA 2005-3572 (2005)